



HHS Public Access

Author manuscript

Stem Cells. Author manuscript; available in PMC 2017 October 01.

Published in final edited form as:

Stem Cells. 2016 October ; 34(10): 2501–2511. doi:10.1002/stem.2435.

Glycoengineering of E-selectin ligands by intracellular versus extracellular fucosylation differentially affects osteotropism of human mesenchymal stem cells

Brad Dykstra^{1,2,*}, Jungmin Lee^{3,4,*}, Luke J. Mortensen^{5,*}, Haixiao Yu⁶, Zhengliang L. Wu⁶, Charles P. Lin⁷, Derrick J. Rossi^{3,4}, and Robert Sackstein^{1,2,8,†}

¹Department of Dermatology and Harvard Skin Disease Research Center, Brigham and Women's Hospital, Harvard Medical School, Boston MA, USA

²Program of Excellence in Glycosciences, Harvard Medical School, Boston, MA, USA

³Program in Cellular and Molecular Medicine, Division of Hematology/Oncology, Boston Children's Hospital, Harvard Medical School, Boston, MA, USA

⁴Department of Stem Cell and Regenerative Biology, Harvard University, Cambridge, MA, USA

⁵Regenerative Bioscience Center, Rhodes Center for Animal and Dairy Science and College of Engineering, University of Georgia, Athens, Georgia, USA

⁶Bio-techne, R&D Systems, Inc, Minneapolis MN, USA

⁷Advanced Microscopy Program, Center for Systems Biology and Wellman Center for Photomedicine, Massachusetts General Hospital, Harvard Medical School, Boston, MA, USA

⁸Department of Medicine, Brigham and Women's Hospital, Harvard Medical School, Boston MA, USA

Abstract

Human mesenchymal stem cells (MSCs) hold great promise in cellular therapeutics for skeletal diseases but lack expression of E-selectin ligands that direct homing of blood-borne cells to bone marrow. Previously, we described a method to engineer E-selectin ligands on the MSC surface by exofucosylating cells with fucosyltransferase VI (FTVI) and its donor sugar, GDP-Fucose,

[†]Correspondence: Robert Sackstein, M.D., Ph.D. Mailing Address: Harvard Institutes of Medicine, Room 671. 77 Avenue Louis Pasteur, Boston MA 02115. Phone: (617)525-5604. Facsimile: (617)-525-5571. RSackstein@partners.org.

^{*}These authors contributed equally to this work.

Author Contributions: B.D.: Conception and design, collection and/or assembly of data, data analysis and interpretation, manuscript writing; J.L.: Conception and design, collection and/or assembly of data, data analysis and interpretation, manuscript writing; L.J.M.: Conception and design, collection and/or assembly of data, data analysis and interpretation, manuscript writing; H.Y.: Provision of study material or patients; Z.L.W.: Provision of study material or patients; C.P.L.: Data analysis and interpretation, manuscript writing; D.J.R.: Data analysis and interpretation, manuscript writing; R.S.: Conception and design, data analysis and interpretation, manuscript writing, final approval of manuscript.

Disclosure of Potential Conflicts of Interest

According to National Institutes of Health policies and procedures, the Brigham & Women's Hospital has assigned intellectual property rights regarding HCELL and GPS to RS, and RS has licensed portions of this technology to an entity he has founded (Warrior Therapeutics, LLC). RS's ownership interests were reviewed and are managed by the Brigham & Women's Hospital and Partners HealthCare in accordance with their conflict of interest policy. RS serves as a consultant to DaVinci Biosciences and to Mesoblast, Inc, and portions of the GPS technology have been licensed to Mesoblast, Inc and to Bio-techne, Inc. DJR is a founder of Moderna Therapeutics, a Cambridge, Massachusetts company that is developing modified-mRNA therapeutics.

enforcing transient surface expression of the potent E-selectin ligand HCELL with resultant enhanced osteotropism of intravenously administered cells. Here, we sought to determine whether E-selectin ligands created via FTVI-exofucosylation are distinct in identity and function to those created by FTVI expressed intracellularly. To this end, we introduced synthetic modified mRNA encoding FTVI (*FUT6*-modRNA) into human MSCs. FTVI-exofucosylation (i.e., extracellular fucosylation) and *FUT6*-modRNA transfection (i.e., intracellular fucosylation) produced similar peak increases in cell surface E-selectin ligand levels, and shear-based functional assays showed comparable increases in tethering/rolling on human endothelial cells expressing E-selectin. However, biochemical analyses revealed that intracellular fucosylation induced expression of both intracellular and cell surface E-selectin ligands and also induced a more sustained expression of E-selectin ligands compared to extracellular fucosylation. Notably, live imaging studies to assess homing of human MSC to mouse calvarium revealed more osteotropism following intravenous administration of intracellularly-fucosylated cells compared to extracellularly-fucosylated cells. This study represents the first direct analysis of E-selectin ligand expression programmed on human MSCs by FTVI-mediated intracellular versus extracellular fucosylation. The observed differential biologic effects of FTVI activity in these two contexts may yield new strategies for improving the efficacy of human MSCs in clinical applications.

Graphical Abstract

Two complimentary approaches were used to create E-selectin ligands on human mesenchymal stem cells (MSC) using fucosyltransferase VI (FTVI): extracellularly, by treating cells with purified FTVI enzyme, and intracellularly, by transfecting cells with FTVI-encoding modified mRNA. The extent to which the newly created E-selectin ligands could improve MSC homing to bone was tested using in vivo calvarial imaging. This three-dimensional reconstruction of a xenotransplanted mouse calvarium region shows bone (grey) and blood vessels (red), 24 hours after intravenously co-transplanting fucosylated MSCs (blue) and control MSCs (green). Both fucosylation approaches significantly increased homing of MSCs to the bone marrow, but intracellularly fucosylated (*FUT6*-mod) MSCs demonstrated increased extravasation into bone marrow parenchyma compared to their exofucosylated counterparts (FTVI-exo). The observed differential biologic effects of FTVI activity in these two contexts may yield new strategies for improving the efficacy of human MSCs in clinical applications. **p<0.01

Key Terms

Mesenchymal Stromal Cell; HCELL; GPS; E-Selectin; sialyl Lewis X; Fucosyltransferase; Exofucosylation; modified mRNA; Intravital Microscopy

Introduction

Mesenchymal stem cells (MSCs) hold much promise for cell therapy due to their convenient isolation and amplification *in vitro*, multi-lineage differentiation ability, tissue-repairing trophic effects, and potent immunomodulatory capacity [1, 2]. In particular, because MSCs are precursors of bone-forming osteoblasts, these cells have drawn great interest for treatment of systemic bone diseases such as osteoporosis or osteogenesis imperfecta.

However, to achieve this goal, it is first necessary to optimize osteotropism of intravascularly administered MSCs.

Recruitment of circulating cells to bone is dependent on E-selectin receptor/ligand adhesive interactions. E-selectin is a calcium-dependent lectin that is expressed constitutively on marrow microvessels, and inducibly expressed on microvessels at inflammatory sites [3–5]. E-selectin prototypically binds a sialofucosylated terminal tetrasaccharide motif known as sialyl Lewis X (sLe^X; NeuAc- α (2,3)-Gal- β (1,4)-[Fuc- α (1,3)]GlcNAc-R). sLe^X can be displayed at the terminal end of glycan chains that modify specific cell surface glycoproteins such as PSGL-1, CD43, or CD44. When sLe^X is displayed by these proteins, they can function as the E-selectin ligands CLA, CD43E or HCELL, respectively [6, 7]. These structures are expressed at high levels on hematopoietic stem and progenitor cells (HSPCs) and other hematopoietic cells, but are completely absent on MSCs. In part due to this deficiency of E-selectin ligands, only a small fraction of injected MSCs home to the bones upon intravenous transplantation [8–10].

The glycan modifications necessary to create E-selectin ligands are performed in the Golgi by specific glycosyltransferases acting in a stepwise fashion. Human MSCs express high levels of CD44, as well as glycosyltransferases required for synthesis of sLe^X, with the notable exception being a complete lack of expression of any of the fucosyltransferases that mediate α -(1,3)-fucosylation: FTIII, FTIV, FTV, FTVI, or FTVII [11]. As such, MSCs express CD44 at the cell surface that is decorated with terminal sialylated lactosamines (NeuAc- α (2,3)-Gal- β (1,4)-GlcNAc-R), requiring only the addition of an α -(1,3)-fucose to be converted into the potent E-selectin ligand HCELL. Previously, we developed a method to modify glycans on the surface of MSCs to create E-selectin ligands by incubating intact cells with purified α -(1,3)-fucosyltransferase enzyme FTVI and its nucleotide sugar donor GDP-fucose. This method, termed ‘glycosyltransferase mediated stereosubstitution’ (GPS), results in the temporary creation of E-selectin ligands (primarily HCELL) on the MSC cell surface. Such FTVI-driven exofucosylation of MSCs has been demonstrated to robustly enhance E-selectin-mediated tethering and rolling on endothelial cells, and, in preclinical studies, has engendered MSC osteotropism (i.e., homing to bone) [7]. Based in part on these results, the efficacy of this approach is now being investigated in a clinical trial using exofucosylated MSCs for treatment of osteoporosis [NCT02566655, clinicaltrials.gov].

In an alternative approach, fucosyltransferase enzyme can be generated intracellularly by introducing synthetic modified mRNA (modRNA) [12, 13]. Similar to exofucosylation, the resultant effects are temporary, enabling the MSCs to return to their natural state after homing. However, the modRNA approach is distinct because it utilizes the MSC’s own cellular machinery to produce the fucosyltransferase enzyme, with access to intracellular stores of GDP-Fucose. Furthermore, endogenous FTVI is membrane-bound and anchored in the Golgi membrane, while purified FTVI used for exofucosylation is soluble, consisting of only the stem and catalytic domains of the protein. Unresolved biological questions about the modRNA approach remain, especially since the Golgi localization could enable enzyme access to acceptors that differ from those accessible to fucosylation on the cell surface. As such, it is unknown whether the E-selectin ligands created by exofucosylation are similar in

identity and function to those that would be created by the action of intracellular fucosyltransferase. Furthermore, the kinetics by which newly synthesized E-selectin ligands are displayed on (and subsequently disappear from) the MSC surface are likely different from that of exofucosylated MSCs. Most importantly, it is not known whether such differences would lead to dissimilarity in the E-selectin ligand-mediated functional abilities of these cells to home to bone marrow.

To address these questions, we undertook a direct comparison between intracellular and extracellular fucosylation using the same alpha-(1,3)-fucosyltransferase in a human cell natively devoid of such enzymes. To this end, using multiple primary cultures of human MSCs, we utilized modRNA to transiently produce FTVI protein in human MSCs, and compared the biochemical and functional properties of the resulting E-selectin ligands with those created via FTVI exofucosylation. Furthermore, we directly compared the *in vivo* homing properties of both types of treated cells by performing *in vivo* imaging of transplanted MSCs in mouse calvarium. This in-depth comparison of FTVI-mediated intracellular versus extracellular fucosylation provides critical information on the activity and function of fucosyltransferase VI in programming cell migration, providing key insights regarding the most appropriate fucosylation approach for clinical utility.

Materials and Methods

Isolation and culture of human mesenchymal stem cells

Human cells were obtained and used in accordance with the procedures approved by the Human Experimentation and Ethics Committees of Partners Cancer Care Institutions (Massachusetts General Hospital, Brigham and Women's Hospital, and Dana-Farber Cancer Institute). Discarded bone marrow filter sets were obtained from normal human donors. Bone marrow cells were flushed from the filter set using PBS plus 10 U/ml heparin (Hospira). The mononuclear fraction was isolated using density gradient media (Ficoll-Histopaque 1.077, Sigma-Aldrich) and suspended at $2-5 \times 10^6$ cells/ml in MSC medium (DMEM 1 g/L glucose, 10% FBS from selected lots, 100 U/ml penicillin, 100 U/ml streptomycin). 20ml of cell suspension was seeded into T-175 tissue culture flasks and incubated at 37°C, 5% CO₂, >95% humidity. 24 hours later, non-adherent cells were removed, the flask was rinsed with PBS, and fresh MSC medium was added. Subsequently, MSC media was exchanged 2x per week. By 1–2 weeks, clusters of adherent MSCs were observed. When confluence approached 80%, cells were harvested and diluted 3- to 5- fold in MSC media and plated into new flasks. To harvest, MSCs were rinsed 2x with PBS, and lifted with 0.05% trypsin and 0.5 mM EDTA. After centrifugation, the cell pellet was resuspended in MSC medium for passaging or washed with PBS for experimental use.

MSC Characterization and Differentiation

MSCs were characterized by FACS staining for a panel of markers, including CD29, CD31, CD34, CD45, CD73, CD90, CD105, CD106, and CD166. Cell viability was measured using Trypan Blue exclusion. To induce osteogenic differentiation, cells were cultured in the presence of MSC media plus 10 nM dexamethasone, 10mM glycerophosphate, and 50µg/ml L-ascorbate-2-phosphate. After 4 days, the L-ascorbate-2-phosphate was removed, and the

media was changed every 3–4 days for a total of 14 days. To induce adipogenic differentiation, cells were cultured in DMEM with 3 ug/L glucose, 3% FBS, 1 μ M dexamethasone, 500 μ M methylisobutylmethylxanthine (IBMX), 33 μ M biotin, 5 μ M rosiglitazone, 100 nM insulin, and 17 μ M pantothenate. After 4 days, the IBMX and rosiglitazone was removed, and the media was changed every 3–4 days for a total of 14 days. As negative control, MSCs were maintained in MSC media, changing every 3–4 days for a total of 14 days. To visualize calcified deposits indicative of osteogenic differentiation, cells were stained with 2% Alizarin Red. After photomicrographs were taken, the cells were destained using 10% cetylpyridinium chloride monohydrate and the stained eluates were measured using a spectrophotometer at 595 nm. To visualize lipid deposits indicative of adipogenic differentiation, cells were stained with 0.3% Oil Red O, and micrographs were taken.

Modified mRNA synthesis

Modified mRNA (modRNA) was synthesized as described previously [14]. Briefly, cDNA encoding human Fucosyltransferase 6 (*FUT6*) was sub-cloned into a vector containing T7 promoter, 5' UTR and 3' UTR. PCR reactions were performed to generate template for in vitro transcription with HiFi Hotstart (KAPA Biosystems). 1.6 μ g of purified PCR product including *FUT6* ORF and 5' and 3' UTR was used as template for RNA synthesis with MEGAscript T7 kit (Ambion). 3'-O-Me-m⁷G(5')ppp(5')G ARCA cap analog (New England Biolabs), adenosine triphosphate and guanosine triphosphate (USB), 5-methylcytidine triphosphate and pseudouridine triphosphate (TriLink Biotechnologies) were used for in vitro transcription reaction. modRNA product was purified using MEGAclean spin columns (Ambion), and aliquots were stored frozen for future use. Nuclear destabilized EGFP (ndGFP) modRNA was similarly prepared as a negative control.

modRNA transfection

modRNA transfections were carried out with Stemfect (Stemgent) as per manufacturer's instructions. Tubes were prepared with 1 μ g of modRNA in 60 μ l of buffer and 2 μ l of reagent in 60 μ l of buffer, then the two complexes were mixed together and incubated for 15 minutes at room temperature. The mixture was added to 1×10^6 MSCs in 2ml of MSC medium. Subsequent to modRNA transfection, the B18R interferon inhibitor (eBioscience) was used as a media supplement at 200 ng/ml.

FTVI production and specific activity measurement

Recombinant FTVI enzyme was produced in CHO cells by established techniques [15], using cDNA encoding amino acids 35-359 of the FTVI protein sequence; this sequence omits the cytoplasmic and transmembrane regions of FTVI, and encompasses the entire stem and catalytic domain of the enzyme. The specific activity of the purified enzyme was determined using the Glycosyltransferase Activity Kit (R&D Systems), as per the manufacturer's instructions. Briefly, 0.1 μ g of recombinant FTVI, 1 μ l of ENTPD3/CD39L3 phosphatase, 15 nmol of N-acetyl-D-lactosamine (V-labs Inc), and 4 nmol of GDP-Fucose (Sigma-Aldrich) were mixed in 50 μ l reaction buffer (25 mM Tris, 10 mM CaCl₂ and 10 mM MnCl₂, pH 7.5) and incubated in a 96-well plate at 37°C for 20 minutes. A second reaction that contained the same components except the recombinant FTVI was

performed as a negative control. Reactions were terminated by the addition of 30 μL of Malachite Green Reagent A and 100 μL of water to each well. Color was developed by the addition of 30 μL of Malachite Green Reagent B to each well followed by gentle mixing and incubation at room temperature for 20 minutes. The plate was read at 620 nm using a multi-well plate reader. Phosphate standards were used to generate a calibration curve, and the specific activity of the FTVI enzyme was determined to be 60 pmol/min/ μg .

FTVI exofucosylation

MSCs were harvested, washed 2x with PBS, and resuspended at 2×10^7 cells/ml in FTVI reaction buffer, containing 20mM HEPES (Gibco), 0.1% human serum albumin (Sigma), 1mM GDP-fucose (Carbosynth), and 60 $\mu\text{g}/\text{ml}$ purified FTVI enzyme in Hank's Balanced Salt Solution (HBSS). Cells were incubated at 37°C for 1 hour. For some experiments, "buffer only" controls were performed in an identical fashion but excluding the FTVI enzyme and GDP-fucose from the reaction. After the reaction, the cells were washed 2x with PBS and used immediately for downstream experiments.

Flow cytometry

2.5 μl HECA-FITC (Biolegend) or CsLex1-FITC (eBiosciences) were added to individual wells of 96-well plates. MSCs were harvested and suspended at $1 \times 10^6/\text{ml}$ in PBS plus 2% FBS, and 50 μl of cell suspension was added to each well. After 30 minutes incubation at 4°C, the plate was washed with 200 μl PBS per well and resuspended in 200 μl PBS. Fluorescence intensity was determined using a Cytomics FC 500 MPL flow cytometer (Beckman Coulter).

Time course of enforced sLe^x expression following FUT6-modRNA transfection and FTVI exofucosylation

MSCs were *FUT6*-modRNA transfected, FTVI exofucosylated, or left untreated, and an aliquot was removed for flow cytometric analysis for expression of sLe^x using mAb HECA452. Remaining cells were passaged into T-25 flasks (6 flasks per group). At 24 hour intervals, one flask from each group was harvested and flow cytometry was performed using HECA452. A time course of cell surface sLex expression was obtained by comparing the mean fluorescence intensity of HECA452 staining on each sample from day to day.

Cell surface neuraminidase treatment and Western blot analysis

Untreated, *FUT6*-modRNA transfected MSCs (day 3), and exofucosylated MSCs (day 0) MSCs were suspended at 10^7 cells/ml in HBSS + 0.1% BSA and incubated with or without 0.1 U/ml of *Arthrobacter ureafaciens* neuraminidase (Sigma) for 45 minutes at 37°C. MSCs were then washed, counted, pelleted and frozen at -80°C. Prior to use, lysates were prepared by adding 30 μl of 2x reducing SDS-Sample Buffer per 10^5 cells and boiling for 10 minutes. The samples were then separated on 7.5% Criterion Tris-HSC SDS-PAGE gels and transferred to PVDF membrane. Membranes were blocked with 5% milk and then stained consecutively with mouse E-selectin human-Ig chimera (E-Ig, R&D Systems), rat anti-mouse E-selectin (clone 10E9.6, BD Biosciences), and goat anti-rat IgG conjugated to horseradish peroxidase (HRP, Southern Biotech). All staining and washes were performed in

Tris-buffered saline plus 0.1% Tween[®]20 plus 2 mM CaCl₂. Blots were visualized with chemiluminescence using Lumi-Light Western Blotting Substrate (Roche) as per the manufacturer's instructions. To confirm equal loading, membranes were subsequently stained with rabbit anti-human beta-actin (ProSci) followed by goat anti-rabbit IgG-HRP (SouthernBiotech), and visualized with chemiluminescence as described.

Immunoprecipitation and E-selectin (E-Ig) pulldown of HCELL

MSCs were *FUT6*-modRNA transfected, FTVI exofucosylated, or untreated (control), and lysates were prepared in 2%NP40, 150mM NaCl, 50mM Tris-HCl (pH7.4), 20µg/mL PMSE, and 1x protease inhibitor cocktail (Roche). Cell lysates were precleared with protein G-agarose beads (Invitrogen). For CD44 immunoprecipitation, lysates were incubated with a cocktail of mouse anti-human CD44 monoclonal antibodies consisting of 2C5 (R&D Systems), F10-44.2 (Southern Biotech), 515 and G44-26 (both from BD Biosciences). For E-selectin pulldown, lysates were incubated with mouse E-Ig in the presence of 2mM CaCl₂. CD44 immunoprecipitates and E-Ig pulldowns were collected with protein G-agarose beads and eluted via boiling in 1.5x reducing SDS-Sample Buffer, run on an SDS-PAGE gel, and Western Blotted with anti-CD44 antibodies 2C5, G44-26, and F10-44.2, or the anti-sLe^x antibody HECA452.

Cell surface protein isolation

MSCs were biotinylated in-flask and cell surface proteins were isolated using the Pierce Cell Surface Protein Isolation Kit (Thermo Scientific), according to the manufacturer's instructions. Briefly, untreated MSCs or *FUT6*-modRNA transfected MSCs plated 3 days prior were rinsed with PBS, and 10 ml of amine-reactive EZ-Link Sulfo-NHS-SS-Biotin reagent was added to each flask. Flasks were gently agitated for 30 minutes at 4°C, and the reaction was quenched with lysine. Cells were harvested, and a portion of the untreated MSCs were exofucosylated with FTVI. After the exofucosylation reaction, cells were washed and lysed. Biotinylated cell surface proteins were isolated using the NeutrAvidin Agarose beads and the spin columns provided in the kit. The flow-through was collected as the non-biotinylated fraction, and the bound proteins were eluted and collected as the biotinylated (cell surface) fraction. These fractions were run on a gel and Western Blot was performed for E-Ig chimera and beta-actin as described.

Parallel plate flow chamber studies

Parallel plate flow experiments were performed using a Bioflux-200 system and 48-well low-shear microfluidic plates (Fluxion Biosciences). Microfluidic chambers were coated with 250 µg/ml fibronectin (BD Biosciences) and seeded with human umbilical vein endothelial cells (HUVECs, Lonza), then cultured in endothelial growth media prepared from the EGM-2 BulletKit (EGM-2 media, Lonza) until confluent monolayers were formed. Four hours prior to assay, HUVECs were activated with 40 ng/ml rhTNF-α (R&D Systems) to induce E-selectin expression. *FUT6*-modRNA transfected MSCs, FTVI exofucosylated MSCs, or untreated MSCs were suspended at 1.0–1.5×10⁶/ml in EGM-2 media and infused initially at a flow rate representing shear stress of 0.5 dynes/cm², increasing at 1-minute intervals to 1, 2, 4, 8, and 16 dynes/cm². The number of rolling cells captured per field was counted for two separate 10-second intervals at each flow rate, and averaged. Cell counts

were corrected for starting cell number by visually determining the total number of cells visible per field in the initial infusate at 0.5 dynes/cm², and expressing the captured cell numbers as a proportion of the starting cell number normalized to the number of cells at 1.0×10⁶ cells/ml. Data is thus presented as the number of rolling cells captured per mm², normalized to 1×10⁶ cells/ml infusate. To determine the specificity of binding of the fucosylated cells, negative controls were performed using HUVECs not activated with TNF- α , and also with activated HUVECs blocked with anti-CD62E (E-selectin) antibody (clone 68-5H11, BD Pharmingen). The blocking antibody was suspended at 20 μ g/ml in EGM-2 media, infused onto the HUVECs and incubated for 20 minutes prior to washing and infusing the fucosylated MSCs. Rolling velocities were calculated by measuring the distance travelled in each 10 second interval for all rolling cells, converting to velocities measured in μ m/second, and reporting the average rolling velocity for all rolling cells at each shear stress.

Vital dye staining and intravenous infusion of human MSC into mice

MSCs were harvested, transfected with *FUT6*-modRNA or nd*GFP*modRNA, and plated into T-175 flasks with B18R. Untreated MSCs were passaged at the same time. 2 days later, the untreated MSCs were harvested and split into FTVI-exofucosylation or “buffer only” control groups. *FUT6* and nd*GFP*transfected MSCs were harvested directly. Aliquots of all samples were removed for flow cytometry analysis of HECA452. MSCs from each of the four treatments were split in two, suspended at 1×10⁶ cells/ml in PBS + 0.1% BSA and stained with 10 μ M Vybrant[®] DiD or Vybrant[®] DiI dyes (Molecular Probes) for 20 minutes at 37°C. Cells were washed twice, and 1:1 reciprocal mixtures (*FUT6*-modRNA transfected MSCs mixed 1:1 with ndGFP control transfected MSCs, and FTVI-exofucosylated MSCs mixed 1:1 with buffer control treated MSCs) were prepared. Pairs of immunocompetent BL/6 mice were retro-orbitally injected with each cell combination, with the membrane dye combination swapped between the mice in each pair. Subsequently, 2 nmol of Angiosense 750 (PerkinElmer) was injected per mouse to enable simultaneous visualization of blood vessels. Aliquots of the cell mixtures injected into each mouse were stained with HECA452-FITC and imaged on a glass slide to confirm the efficacy of the *FUT6*-mod or FTVI-exo treatment. A minimum of 20 such images (average 450 cells) were counted to provide a precise starting ratio of DiD and DiI labeled MSCs for each mouse. In cases where the starting ratio was different from 1:1, a correction factor was calculated and the homing ratios obtained from the in vivo images were adjusted accordingly.

In vivo confocal and 2-photon fluorescence microscopy

MSC homing to the *in vivo* calvarial bone marrow was imaged using a custom-built video-rate laser-scanning microscope designed for live animal imaging under isoflurane anesthesia. Scalp hair was shaved, and a skin flap was surgically opened, exposing the calvarium. The calvarial region was wetted with saline and positioned directly under a 60x 1.0NA water immersion objective lens (Olympus, Center Valley, PA). Image stacks were acquired at 30 frames per second, with frame averaging to enhance the signal-to-noise ratio. DiI-labeled MSCs, DiD-labeled MSCs, and Angiosense 750-labeled vasculature were imaged using a confocal detection scheme. Second harmonic generation of bone collagen was performed using 840 nm light from a femtosecond pulsed Maitai laser (Coherent, Inc., Santa Clara, CA). Cells could be detected to a depth of approximately 200 μ m in the tissue. Imaging was

performed at ~2 hours and ~24 hours post-transplant. Between imaging sessions, the scalp flap was stitched closed and the mouse was allowed to recover. Studies were in accordance with U.S. National Institutes of Health guidelines for care and use of animals under approval of the Institutional Animal Care and Use Committees of Massachusetts General Hospital.

In vivo image analysis

Calvarial images were collected and quantified as 3-dimensional stacks [16]. For quantification, the numbers of DiD and DiI cells in 20 representative imaging locations across the bone marrow of the calvarium were manually counted for each mouse. Analysis was performed blinded, with counted events corresponding to a minimum diameter of ~10 μm to eliminate debris from analysis, and excluding autofluorescent events with signal in both DiD and DiI channels (those events with the intensity of the primary channel less than ~2x the intensity of the other channel). Extravasated cells were defined as those that were completely discrete from the Angiosense labeled vessels (i.e. no part of the cell was overlapping with any part of any vessel). The ratios of DiD to DiI stained cells counted in each mouse were calculated and compared within each mouse pair, with equivalent homing assigned a baseline ratio of 1. Fold change in homing of the treated MSCs compared to control MSCs was thus calculated for each pair of mice to provide a relative measurement of homing efficacy. 8 mice (4 mouse pairs) representing 4 different primary MSC lines were imaged per treatment.

Results

MSC characterization

Primary bone marrow-derived MSCs were assessed for a panel of markers, including CD29, CD31, CD34, CD45, CD73, CD90, CD105, CD106, and CD166. The MSCs were uniformly positive for the MSC markers CD29, CD44, CD73, CD90 and CD105, were dim for CD106, and were negative for the endothelial cell marker CD31 and the hematopoietic markers CD34 and CD45 (Supplementary Fig. 1A). This marker expression profile was consistent across all 7 primary MSC lines tested (Supplementary Fig. 1B). Two primary MSC lines were tested for the ability to differentiate towards adipogenic and osteogenic lineages (representative images shown in Supplementary Fig. 1C).

sLe^x surface expression peaks 2–3 days after FUT6-modRNA transfection and declines more slowly than with FTVI exofucosylation

To determine the optimal time point for cell surface E-selectin ligand expression, we compared the kinetics of sLe^x surface expression between FTVI exofucosylation and *FUT6*-modRNA transfection of MSCs by flow cytometry. As expected, the exofucosylated cells had maximal surface sLe^x immediately after treatment, decreased to 40% by 24 hours, and returned a baseline level of near zero (i.e., similar to native MSC reactivity) by 48 hours. In contrast, the *FUT6*-modRNA transfected cells reached maximal cell surface sLe^x expression at day 2 post-transfection, with high levels maintained until day 3, followed by gradual decrease thereafter (Fig. 1). Based on these kinetics of induced sLe^x expression, all experiments with exofucosylated cells were performed just after treatment, whereas

experiments with *FUT6*-modRNA-transfected cells were performed 2–3 days post-transfection.

sLe^x surface expression induced by intracellular and extracellular FTVI fucosylation is similar and consistent across multiple primary MSC lines, and does not alter MSC properties

To evaluate the overall extent of fucosylation of cell surface glycans using both methods, we analyzed total cell surface sLe^x levels by flow cytometry. This analysis revealed an approximately two-log increase in surface sLe^x expression in both intracellularly and extracellularly fucosylated cells (Fig. 2A), results that were confirmed using a second anti-sLe^x mAb clone to exclude clone-specific bias (Fig. 2A). Although some variability between MSC primary cultures was observed, on average the increase in cell surface sLe^x was similar for both methods when tested in 5 independent primary MSC lines (Fig. 2B).

To determine whether either method of FTVI fucosylation affected characteristic MSC biology, we examined several key properties before and after fucosylation (Supplementary Fig. 2). We observed that MSC viability was not significantly decreased by intracellular or extracellular fucosylation (Supplementary Fig. 2A), and that a panel of MSC markers did not change, either when measured immediately after fucosylation (Supplementary Fig. 2B, 2C) or when cultured for an additional passage (i.e. 5–11 days) (Supplementary Fig. 2C). Finally, we differentiated the treated cells towards osteoblastic and adipogenic lineages, and no visual differences in differentiation could be observed. Quantification of osteoblastic differentiation revealed no significant difference between the intracellularly and extracellularly fucosylated MSCs and their respective controls, and no decrease compared to untreated MSCs (Supplementary Fig. 2D).

Comparative analysis of E-selectin ligand glycoproteins created by intracellular and extracellular fucosylation

To analyze the identity and cellular localization of the E-selectin ligand glycoproteins created by *FUT6*-modRNA transfection and FTVI-exofucosylation, we performed western blot using an E-selectin-Ig chimera (E-Ig) as a probe. Lysates from extracellularly fucosylated MSCs exhibited E-Ig reactive bands predominantly at ~85kD, corresponding in size to HCELL [7], and ~60kD, a currently undefined glycoprotein (Fig. 3A). To assess whether the ~85kD band was indeed HCELL, we immunoprecipitated CD44 and blotted with HECA452, and conversely, isolated E-selectin ligands using E-Ig and blotted with CD44 (Supplementary Fig. 3). Both HCELL and the ~60 kD band were similarly present in lysates of intracellularly fucosylated MSCs, however, E-Ig reactive bands of larger molecular weights were also observed with much greater intensity in these lysates, suggesting that additional glycoprotein substrates are accessible to fucosylation when FTVI is present in its native intracellular context (Fig. 3A). To determine the cellular localization of the E-Ig reactive proteins, neuraminidase treatment of intact cells was performed to remove sLex from all cell surface glycoproteins. As expected, no E-Ig reactive glycoproteins remained after neuraminidase treatment of extracellularly fucosylated cells, indicating that all were localized extracellularly. In intracellularly fucosylated cells (day 3), all detectable E-Ig reactive proteins at ~60kD and ~85kD were extracellular, however, a portion of the

larger E-Ig reactive proteins were still present after neuraminidase treatment, suggesting an intracellular localization (Fig. 3B). This trend was corroborated by cell surface biotinylation experiments, which revealed that the ~60kD and ~85kD bands were over-represented within the accessible cell surface proteins compared to the larger E-Ig reactive proteins (Supplementary Fig. 4).

Intracellular and extracellular fucosylation similarly enable E-selectin ligand-mediated MSC capture, tethering and rolling under fluid shear conditions

Since sLe^x is the critical binding determinant for E-selectin, the dramatic increase in HECA452 and csLex1 reactivity suggests that both intracellular and extracellular fucosylation should enable functional E-selectin binding activity on treated MSCs. To directly assess E-selectin binding activity, we tested the ability of fucosylated and untreated MSCs to capture, tether and roll under fluid shear conditions on HUVEC monolayers stimulated to express E-selectin by treatment with TNF α . Untreated MSCs showed little or no interaction with the stimulated HUVECs at any level of shear stress, consistent with their lack of E-selectin ligand expression. In contrast, both intracellularly and extracellularly fucosylated MSCs were greatly enhanced in their ability to capture, tether and roll on TNF α -stimulated HUVEC monolayers at shear stress levels up to 4 dynes/cm² (Fig. 4A). No significant difference was observed between extracellularly and intracellularly fucosylated MSCs in the number of rolling cells (Fig. 4A) or rolling velocities (Fig. 4B), suggesting that the similar increased levels of surface sLe^x observed by FACS correctly predicted a commensurate functional improvement of the resulting E-selectin ligand activity on the treated MSCs. Non-stimulated HUVECs or HUVECs treated with an anti-E-selectin blocking monoclonal antibody did not support capture, tethering or rolling interactions with fucosylated MSCs, confirming that these interactions were solely E-selectin-mediated.

Both intracellularly and extracellularly fucosylated MSCs accumulate more efficiently in calvarial bone marrow than untreated MSCs

The dramatic increases of cell surface sLe^x observed by FACS, of E-Ig reactivity observed by Western blot, and of capture/tethering and rolling on TNF α stimulated HUVECs collectively indicate both intracellular and extracellular fucosylation can create operational E-selectin ligands on MSCs. To determine whether these differences in E-selectin ligands are functionally relevant *in vivo*, we studied their bone marrow homing properties *in vivo* using intravital confocal and multiphoton microscopy for cell tracking in the calvarium in murine hosts [12, 16]. Intracellularly or extracellularly fucosylated MSCs, together with corresponding non-fucosylated control cells, were each stained with the cell surface dyes DiD or DiI, and 1:1 reciprocal cell mixtures (treated vs control) were prepared. Pairs of mice were transplanted with each cell combination, with the membrane dye combination swapped between the mice in each pair. Aliquots of the cell mixtures injected into each mouse were stained with HECA452 and imaged on a glass slide to confirm the efficacy of fucosylation, and to provide a precise starting ratio (Supplementary Fig. 5). At approximately 2 hours and again at 24 hours post-transplantation, the calvaria were imaged (Fig. 5A), and DiD and DiI events were counted. Compared to control MSCs, both intracellularly and extracellularly fucosylated MSCs demonstrated significantly increased osteotropism (i.e. accumulation in the bone) at 2 hours post-transplantation (Fig. 5B). When the same mice were imaged at 24

hours post-transplantation, a similar trend was observed, with a further significant increase in cell numbers observed with intracellularly fucosylated MSCs compared to intracellularly fucosylated MSCs (Fig. 5C).

Intracellularly fucosylated MSCs demonstrate significantly greater extravasation from calvarial vessels into bone marrow parenchyma at 24 hours post-transplant

Extravasation of transplanted cells into the marrow parenchyma is prerequisite for engraftment. To evaluate the extent of extravasation, we injected a near-infrared vascular dye (Angiosense 750) to visualize mouse blood vessels and performed multi-stack imaging. We imaged the calvaria at 24 hours post-transplantation to identify DiI and DiD stained cells that had clearly extravasated from the vessels into the surrounding bone marrow space (Fig. 6A), and found that compared to control MSCs, both intracellularly and extracellularly fucosylated MSCs showed significantly more penetration into the marrow parenchyma (Fig. 6B). Furthermore, a clear difference in extravasation was observed between the two treatments, with the intracellularly fucosylated MSCs being two-fold more likely to be extravasated than the extracellularly fucosylated MSCs at 24 hours post-transplantation (Fig. 6B). These findings suggest that the sustained presence of E-selectin ligands (i.e., beyond day 2) of *FUT6*-modRNA transduction (Fig. 1) engenders a functional improvement in cell homing and extravasation in an *in vivo* context.

Discussion

MSCs represent an avenue of cell therapy that has great potential for clinical impact. There are over 500 past or current registered clinical trials worldwide utilizing MSCs in efforts to treat a broad range of conditions including bone diseases (e.g. osteoporosis, osteogenesis imperfecta), autoimmune diseases (e.g. lupus, multiple sclerosis), and inflammatory diseases (e.g. myocardial infarction, ulcerative colitis) [clinicaltrials.gov, accessed December 2015]. However, while MSC transplantation has been well tolerated, clinical outcomes have generally been disappointing [2, 17]. A major unresolved challenge limiting the clinical efficacy of MSCs is the effective delivery of transplanted MSCs to their intended target site(s). While direct injection of MSCs into injured/diseased organs is possible for some indications, this approach is invasive and can result in collateral tissue damage. Furthermore, for certain organs or for multifocal or systemic conditions, local injection is not feasible, necessitating strategies to optimize vascular delivery of the cells to enable effective site-specific localization.

One of the primary deficiencies that limit MSC homing is their lack of E-selectin ligand expression. Various approaches have been utilized in attempts to engineer MSCs with E-selectin ligands, including covalent peptide linkage to the cell membrane [18], and non-covalent coupling of an E-selectin ligand fusion protein [19] or sLe^x coated polymer beads [20]. Arguably however, the most physiologically relevant approach is to harness the power of the human alpha (1,3)-fucosyltransferase enzymes, which by their nature are potent and specific in their ability to convert terminal sialylated lactosamines into sLe^x, the canonical selectin binding determinant. We have previously described the use of purified FTVI to exofucosylate the cell surface of MSCs, thus creating the E-selectin ligand HCELL and

improving homing to bone [7]. Exofucosylation has also been employed to enhance selectin-mediated homing and engraftment in other cell types, including umbilical cord hematopoietic cells [21–23], regulatory T-cells [24], and neural stem cells [25]. In contrast, the use of modRNA to generate fucosyltransferase intracellularly in MSCs is new and relatively unexplored. In the only studies to date, human MSCs were co-transfected with modRNAs encoding FTVII, P-selectin glycoprotein ligand-1 (PSGL-1) and the anti-inflammatory cytokine interleukin-10 (IL-10). When these triple-transfected cells were xenotransplanted into mice, a slight enhancement of bone marrow homing was reported, along with a modest improvement in a skin inflammation model [12] and an experimental autoimmune encephalomyelitis model [26]. However, the nature of the experimental design (i.e. co-transfecting modRNAs to express three genes simultaneously), as well as differences in methodology (different fucosyltransferase, different preclinical models) made it difficult to compare the results with those from other studies employing exofucosylation. In particular, it was not possible to determine from these studies whether the E-selectin ligands created by modRNA transfection are similar in identity and function to those that would be created by the action of extracellular fucosyltransferase, and whether any differences in resulting homing efficiency would be realized.

Our results here indicate that, across multiple primary cultures of human MSCs, intracellular and extracellular fucosylation methods are similarly potent for generation of cell surface E-selectin ligands, as measured by sLe^x levels and confirmed by assessing E-selectin-mediated capture/tethering/rolling activity under hemodynamic shear conditions on cytokine-stimulated HUVECs. The amount and cellular location of certain E-selectin ligand glycoproteins produced are slightly different between the two methods, with intracellular fucosylation resulting in some additional E-selectin-binding glycoproteins present both intracellularly and extracellularly. Whether the additional intracellular proteins represent novel sLe^x bearing glycoproteins that are normally localized inside the cell, or are precursors for export of cell surface presentation (i.e. proteins undergoing further post-translational modifications, stored in granules, or in the process of being shuttled to the cell surface) remains to be determined. The most striking differences between the two methods were the kinetics of E-selectin ligand display on the cell surface. Peak sLe^x was observed immediately after extracellular fucosylation with a rapid decline by 1–2 days, whereas, with intracellular fucosylation, sLe^x peaked at 48 hours and declined more gradually thereafter. Additionally, while both methods significantly increased osteotropism compared to control MSCs, a larger increase in overall marrow homing and, particularly, in transmigration, was observed for intracellularly fucosylated cells at 24 hours post-transplant in vivo. Considering the fact that MSCs were injected immediately after exofucosylation or day 2 post-modRNA transfection, it is likely that the markedly different levels of E-selectin ligands remaining on the cell surface 24 hours later contributed to these differences. Additional studies are warranted to determine the molecular basis of this effect, but it could also relate to heightened glycan acceptor accessibility in the Golgi and/or differences in membrane distribution of intracellularly glycosylated products.

Our findings are important for informing future clinical applications using human MSCs. Both FTVI exofucosylation and *FUT6*-modRNA transfection are ideal glycoengineering strategies as they are simple, transient, and non-integrative. In addition to the longer

duration of E-selectin ligand expression after intracellular glycosylation and the associated improvement in homing and transmigration properties described here, a practical advantage of this approach is that the FTVI enzyme and GDP-Fucose are cell products, thereby eliminating the effort and expense associated with the purification of soluble recombinant enzyme and synthesis of GDP-Fucose. Furthermore, since the FTVI enzyme is localized in its native cellular context (i.e., embedded in the Golgi membrane), additional acceptor substrates are accessible for fucosylation. On the other hand, practical advantages to extracellular fucosylation include the rapidity of the treatment (thus avoiding further culture of the cells), the avoidance of potential disruption of Golgi glycosylation networks, and the elimination of risks involved with introducing nucleic acids into cells, including, but not limited to, activation of cellular antiviral defense mechanisms. Furthermore, when considering fucosylation of other (i.e., non-MSC) clinically-relevant cells, exofucosylation is easily applicable to any cell type bearing sialylated lactosamines on its cell surface, in contrast to intracellular fucosylation which is limited to those cell types that are readily transfectable with modRNA. Therefore, depending on the specific clinical application(s), one might favor utility of the intracellular or the extracellular fucosylation approach.

It is now clear that maximizing E-selectin interactions via fucosylation is a valid strategy for improving osteotropism. However, MSCs can also be modified in other ways to further improve homing and differentiation. For example, efforts have been made to improve bone surface retention by affixing alendronate to MSCs [27], improving cell migration into the tissue by upregulating CXCR4 [28–30], and improving firm adhesion and differentiation to bone by increasing integrin levels or activity [31–33]. It seems reasonable that future translational efforts could seek to combine multiple homing and differentiation approaches in a specific and step-wise fashion to enhance MSC engagement at each stage of the homing, engraftment and differentiation process. Fucosylation could thus be used as an important aspect of a combinatorial approach to maximize the clinical utility of MSCs.

Conclusion

Here we report, using multiple primary human MSC lines, a functional and biochemical assessment of two distinct approaches using the alpha (1,3)-fucosyltransferase *FUT6* for transiently increasing cell surface E-selectin ligands, and their impact on MSC homing to bone. This study represents the first direct comparison between intracellular and extracellular fucosylation using the same enzyme in a clinically relevant experimental model. Compared to untreated MSCs, both intracellular and extracellular fucosylation markedly increased cell surface E-selectin ligands and improved osteotropism in all primary MSC lines tested, indicating that these approaches are consistent and relevant across multiple MSC donors. Notably, at 24 hours post-transplant, overall osteotropism and levels of extravasation were significantly higher with intracellular than extracellular fucosylation. This finding is likely a reflection of the more sustained expression and increased diversity of cell surface E-selectin ligands on the intracellularly versus extracellularly fucosylated MSCs. Collectively, these results indicate that this simple and non-permanent strategy to enforce fucosylation could be of use in augmenting homing of transplanted MSCs.

Supplementary Material

Refer to Web version on PubMed Central for supplementary material.

Acknowledgments

The authors thank the MGH Bone Marrow Transplant Cellular Processing Laboratory for provision of discarded bone marrow filters, and Conor Donnelly for expert technical assistance. R.S. is supported by the NIH National Heart Lung Blood Institute (NHLBI) Program of Excellence in Glycosciences (PEG) grant PO1-HL107146, and the Team Jobie Fund. C.L. is supported by NIH R01 EB017274. L.J.M. is supported by the Soft Bones Foundation Maher Family Research Grant and UGA OVPF Faculty Research grant. D.J.R. is supported by grants from the NIH (R01HL107630, HL107440, UC4DK104218, and U19HL129903), the Leona M. and Harry B. Helmsley Charitable Trust, and the New York Stem Cell Foundation.

References

1. Dominici M, Le Blanc K, Mueller I, et al. Minimal criteria for defining multipotent mesenchymal stromal cells. The International Society for Cellular Therapy position statement. *Cytotherapy*. 2006; 8:315–317. [PubMed: 16923606]
2. Griffin MD, Elliman SJ, Cahill E, et al. Adult Mesenchymal Stromal Cell Therapy for Inflammatory Diseases: How Well are We Joining the Dots? *Stem Cells*. 2013
3. Sipkins DA, Wei X, Wu JW, et al. In vivo imaging of specialized bone marrow endothelial microdomains for tumour engraftment. *Nature*. 2005; 435:969–973. [PubMed: 15959517]
4. Schweitzer KM, Dräger AM, van der Valk P, et al. Constitutive expression of E-selectin and vascular cell adhesion molecule-1 on endothelial cells of hematopoietic tissues. *The American Journal of Pathology*. 1996; 148:165–175. [PubMed: 8546203]
5. Sackstein R. Glycosyltransferase-programmed stereosubstitution (GPS) to create HCELL: engineering a roadmap for cell migration. *Immunological Reviews*. 2009; 230:51–74. [PubMed: 19594629]
6. Dimitroff CJ, Lee JY, Rafii S, et al. Cd44 Is a Major E-Selectin Ligand on Human Hematopoietic Progenitor Cells. *The Journal of Cell Biology*. 2001; 153:1277–1286. [PubMed: 11402070]
7. Sackstein R, Merzaban JS, Cain DW, et al. Ex vivo glycan engineering of CD44 programs human multipotent mesenchymal stromal cell trafficking to bone. *Nature Medicine*. 2008; 14:181–187.
8. Schrepfer S, Deuse T, Reichenspurner H, et al. Stem cell transplantation: the lung barrier. *Transplant Proc*. 2007; 39:573–576. [PubMed: 17362785]
9. Lee RH, Pulin AA, Seo MJ, et al. Intravenous hMSCs improve myocardial infarction in mice because cells embolized in lung are activated to secrete the anti-inflammatory protein TSG-6. *Cell Stem Cell*. 2009; 5:54–63. [PubMed: 19570514]
10. Ankrum J, Karp JM. Mesenchymal stem cell therapy: Two steps forward, one step back. *Trends Mol Med*. 2010; 16:203–209. [PubMed: 20335067]
11. Sackstein R. Glycosyltransferase-programmed stereosubstitution (GPS) to create HCELL: engineering a roadmap for cell migration. *Immunol Rev*. 2009; 230:51–74. [PubMed: 19594629]
12. Levy O, Zhao W, Mortensen LJ, et al. mRNA-engineered mesenchymal stem cells for targeted delivery of interleukin-10 to sites of inflammation. *Blood*. 2013; 122:e22–e32.
13. Warren L, Manos PD, Ahfeldt T, et al. Highly efficient reprogramming to pluripotency and directed differentiation of human cells with synthetic modified mRNA. *Cell Stem Cell*. 2010; 7:618–630. [PubMed: 20888316]
14. Mandal PK, Rossi DJ. Reprogramming human fibroblasts to pluripotency using modified mRNA. *Nat Protoc*. 2013; 8:568–582. [PubMed: 23429718]
15. Borsig L, Katopodis AG, Bowen BR, et al. Trafficking and localization studies of recombinant alpha1, 3-fucosyltransferase VI stably expressed in CHO cells. *Glycobiology*. 1998; 8:259–268. [PubMed: 9451035]
16. Mortensen LJ, Levy O, Phillips JP, et al. Quantification of Mesenchymal Stem Cell (MSC) delivery to a target site using in vivo confocal microscopy. *PloS one*. 2013; 8:e78145. [PubMed: 24205131]

17. Galipeau J. The mesenchymal stromal cells dilemma--does a negative phase III trial of random donor mesenchymal stromal cells in steroid-resistant graft-versus-host disease represent a death knell or a bump in the road? *Cytotherapy*. 2013; 15:2–8. [PubMed: 23260081]
18. Cheng H, Byrska-Bishop M, Zhang CT, et al. Stem cell membrane engineering for cell rolling using peptide conjugation and tuning of cell-selectin interaction kinetics. *Biomaterials*. 2012; 33:5004–5012. [PubMed: 22494889]
19. Lo CY, Antonopoulos A, Dell A, et al. The use of surface immobilization of P-selectin glycoprotein ligand-1 on mesenchymal stem cells to facilitate selectin mediated cell tethering and rolling. *Biomaterials*. 2013; 34:8213–8222. [PubMed: 23891082]
20. Sarkar D, Spencer JA, Phillips JA, et al. Engineered cell homing. *Blood*. 2011; 118:e184–191. [PubMed: 22034631]
21. Xia L, McDaniel JM, Yago T, et al. Surface fucosylation of human cord blood cells augments binding to P-selectin and E-selectin and enhances engraftment in bone marrow. *Blood*. 2004; 104:3091–3096. [PubMed: 15280192]
22. Wan X, Sato H, Miyaji H, et al. Fucosyltransferase VII improves the function of selectin ligands on cord blood hematopoietic stem cells. *Glycobiology*. 2013; 23:1184–1191. [PubMed: 23899669]
23. Papat U, Mehta RS, Rezvani K, et al. Enforced fucosylation of cord blood hematopoietic cells accelerates neutrophil and platelet engraftment after transplantation. *Blood*. 2015; 125:2885–2892. [PubMed: 25778529]
24. Parmar S, Liu X, Najjar A, et al. Ex vivo fucosylation of third-party human regulatory T cells enhances anti-graft-versus-host disease potency in vivo. *Blood*. 2015; 125:1502–1506. [PubMed: 25428215]
25. Merzaban JS, Imitola J, Starossom SC, et al. Cell surface glycan engineering of neural stem cells augments neurotropism and improves recovery in a murine model of multiple sclerosis. *Glycobiology*. 2015; 25:1392–1409. [PubMed: 26153105]
26. Liao W, Pham V, Liu L, et al. Mesenchymal stem cells engineered to express selectin ligands and IL-10 exert enhanced therapeutic efficacy in murine experimental autoimmune encephalomyelitis. *Biomaterials*. 2016; 77:87–97. [PubMed: 26584349]
27. Yao W, Guan M, Jia J, et al. Reversing bone loss by directing mesenchymal stem cells to bone. *Stem Cells*. 2013; 31:2003–2014. [PubMed: 23818248]
28. Wynn RF, Hart CA, Corradi-Perini C, et al. A small proportion of mesenchymal stem cells strongly expresses functionally active CXCR4 receptor capable of promoting migration to bone marrow. *Blood*. 2004; 104:2643–2645. [PubMed: 15251986]
29. Shi M, Li J, Liao L, et al. Regulation of CXCR4 expression in human mesenchymal stem cells by cytokine treatment: role in homing efficiency in NOD/SCID mice. *Haematologica*. 2007; 92:897–904. [PubMed: 17606439]
30. Jones GN, Moschidou D, Lay K, et al. Upregulating CXCR4 in human fetal mesenchymal stem cells enhances engraftment and bone mechanics in a mouse model of osteogenesis imperfecta. *Stem Cells Transl Med*. 2012; 1:70–78. [PubMed: 23197643]
31. Kumar S, Ponnazhagan S. Bone homing of mesenchymal stem cells by ectopic alpha 4 integrin expression. *FASEB J*. 2007; 21:3917–3927. [PubMed: 17622670]
32. Srouji S, Ben-David D, Fromigue O, et al. Lentiviral-mediated integrin alpha5 expression in human adult mesenchymal stromal cells promotes bone repair in mouse cranial and long-bone defects. *Hum Gene Ther*. 2012; 23:167–172. [PubMed: 21958321]
33. Hamidouche Z, Fromigue O, Ringe J, et al. Priming integrin alpha5 promotes human mesenchymal stromal cell osteoblast differentiation and osteogenesis. *Proc Natl Acad Sci U S A*. 2009; 106:18587–18591. [PubMed: 19843692]

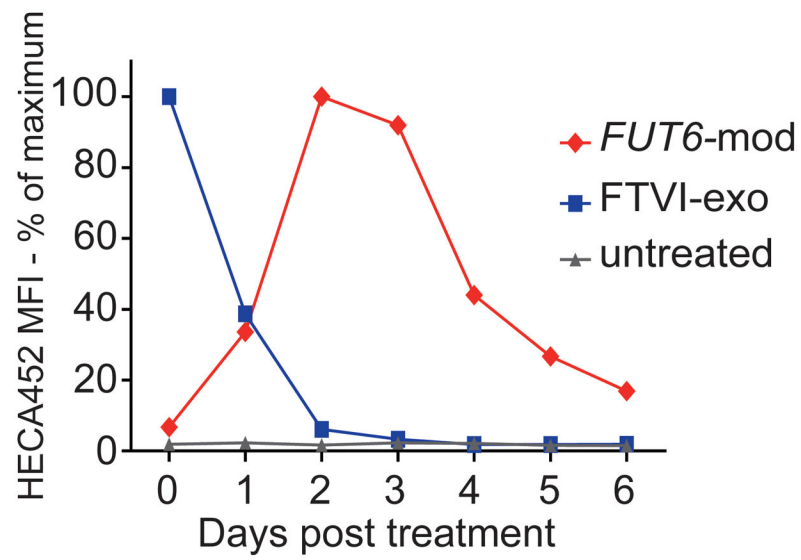


Figure 1. Kinetics of sLe^x surface expression following intracellular or extracellular fucosylation of MSCs

Untreated MSCs, extracellularly fucosylated (FTVI-exo) MSCs, or intracellularly fucosylated (*FUT6-mod*) MSCs were harvested at 24-hour intervals, stained for sLe^x using HECA452 antibody, and analyzed by flow cytometry. MFI: Mean fluorescence intensity.

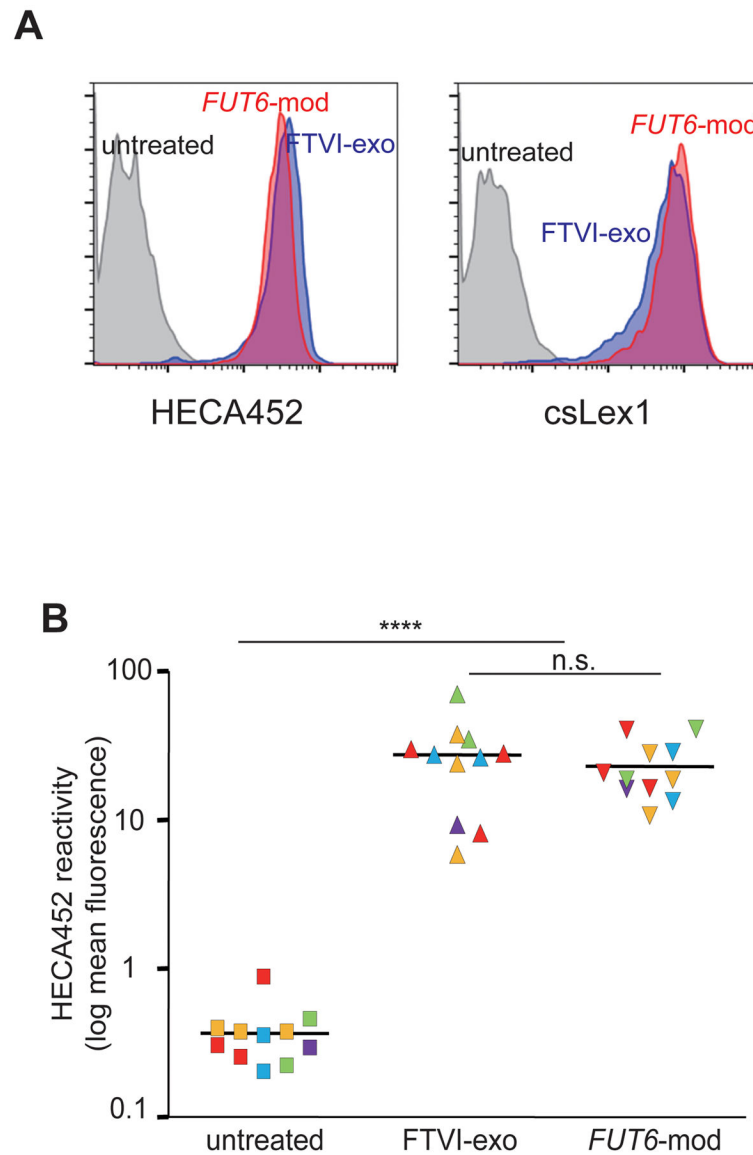


Figure 2. Cell surface sLe^x expression levels induced by intracellular or extracellular fucosylation in multiple primary human MSC lines
 (A) Day 0 extracellularly fucosylated (FTVI-exo) MSCs and day 2–3 intracellularly fucosylated (*FUT6*-mod) MSCs show similar increase in surface sLe^x compared to untreated MSCs, as measured via flow cytometry analysis of HECA452 or csLex1 staining.
 (B) Similar increase in surface sLe^x observed across multiple independent primary MSC lines (n=11 experiments; each color represents 1 of 5 primary MSC lines used). Statistical comparisons made using Student's T-test. n.s.= not significant (i.e. p>0.05). **** indicates p<0.0001.

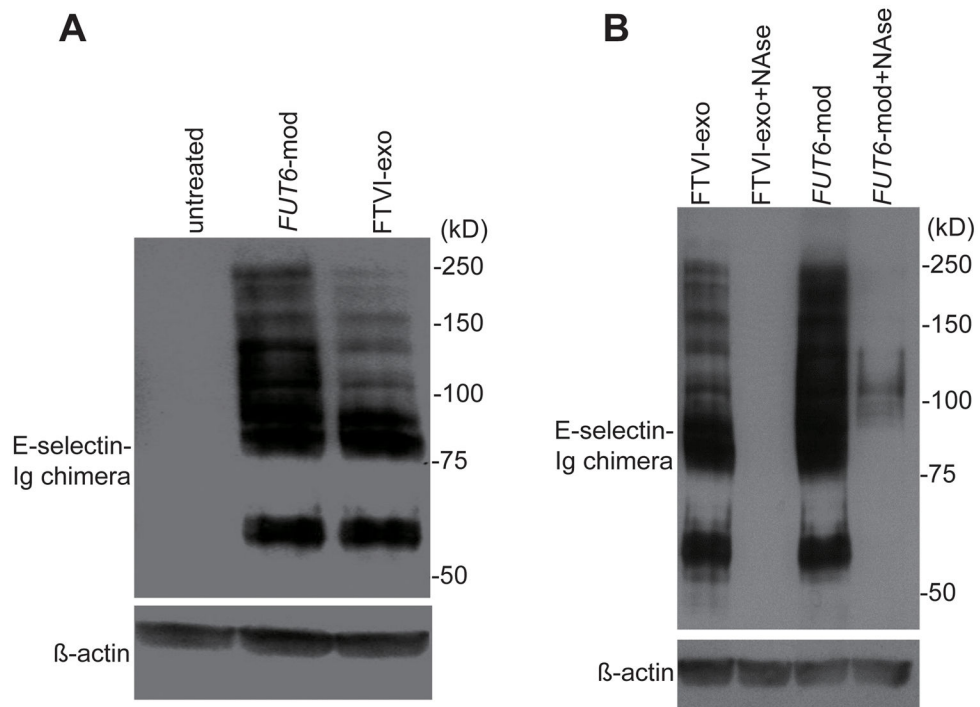


Figure 3. Comparison of protein size and cellular localization of E-selectin ligand glycoproteins created by intracellular or extracellular fucosylation

(A) Untreated MSCs, intracellularly fucosylated (*FUT6*-mod) MSCs, and extracellularly fucosylated (FTVI-exo) MSCs were lysed and Western blotted using mouse E-selectin-human Fc (E-Ig) chimera as a probe. (B) Cellular localization of E-Ig reactive glycoproteins determined by treatment of intact intracellularly or extracellularly fucosylated MSCs with or without neuraminidase (Nase) prior to cell lysis and E-Ig Western blot. β -actin staining of same blots were performed as loading control.

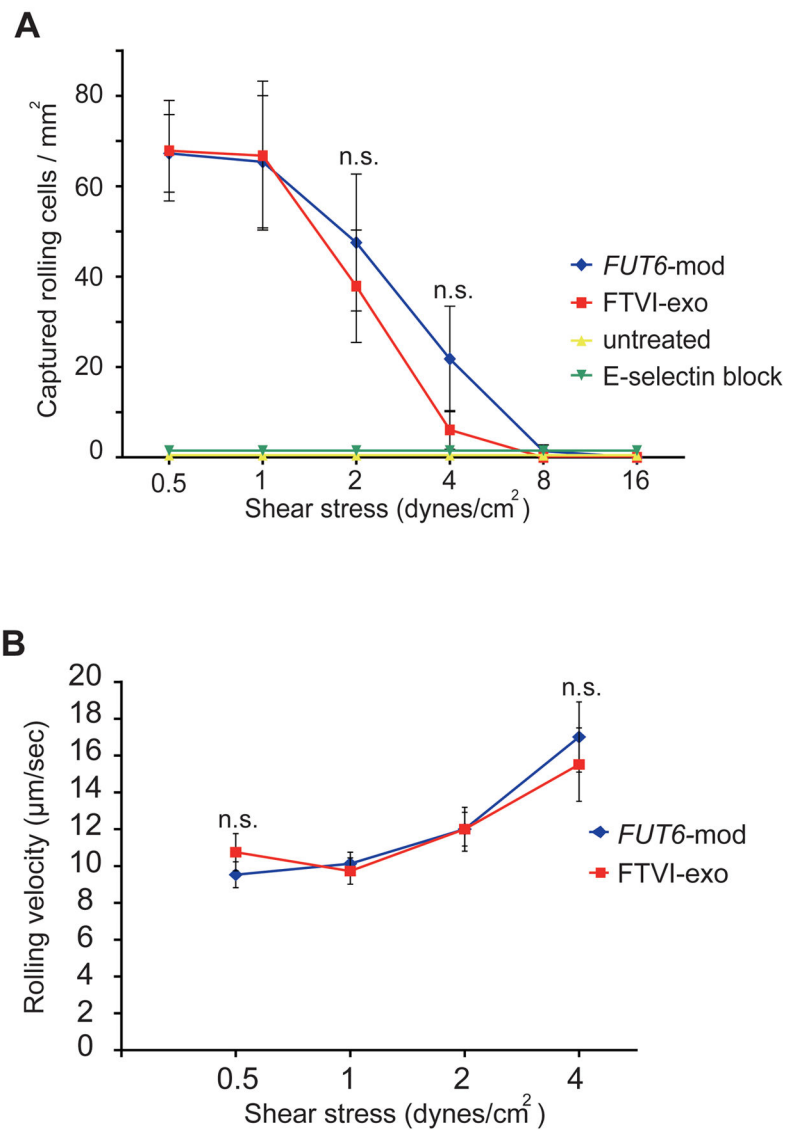


Figure 4. Analysis of E-selectin ligand mediated MSC-endothelial cell interactions under shear conditions using parallel plate flow chamber

(A) Both extracellular fucosylation (FTVI-exo) and intracellular fucosylation (*FUT6*-mod) enabled MSC capture/tethering/rolling under flow conditions on TNF α -activated human umbilical vein endothelial cells (HUVECs), but not on HUVECs pretreated with an anti-E-selectin function-blocking mAb. Error bars = SEM, n=4 independent experiments using 2 different primary MSC lines. (B) Extracellularly fucosylated and intracellularly fucosylated MSCs show similar rolling velocities on TNF α -stimulated HUVECs. Error bars = SEM, n=15 to 155 cell velocities analyzed per time point. Statistical comparisons made using Student's T-test. n.s.= not significant.

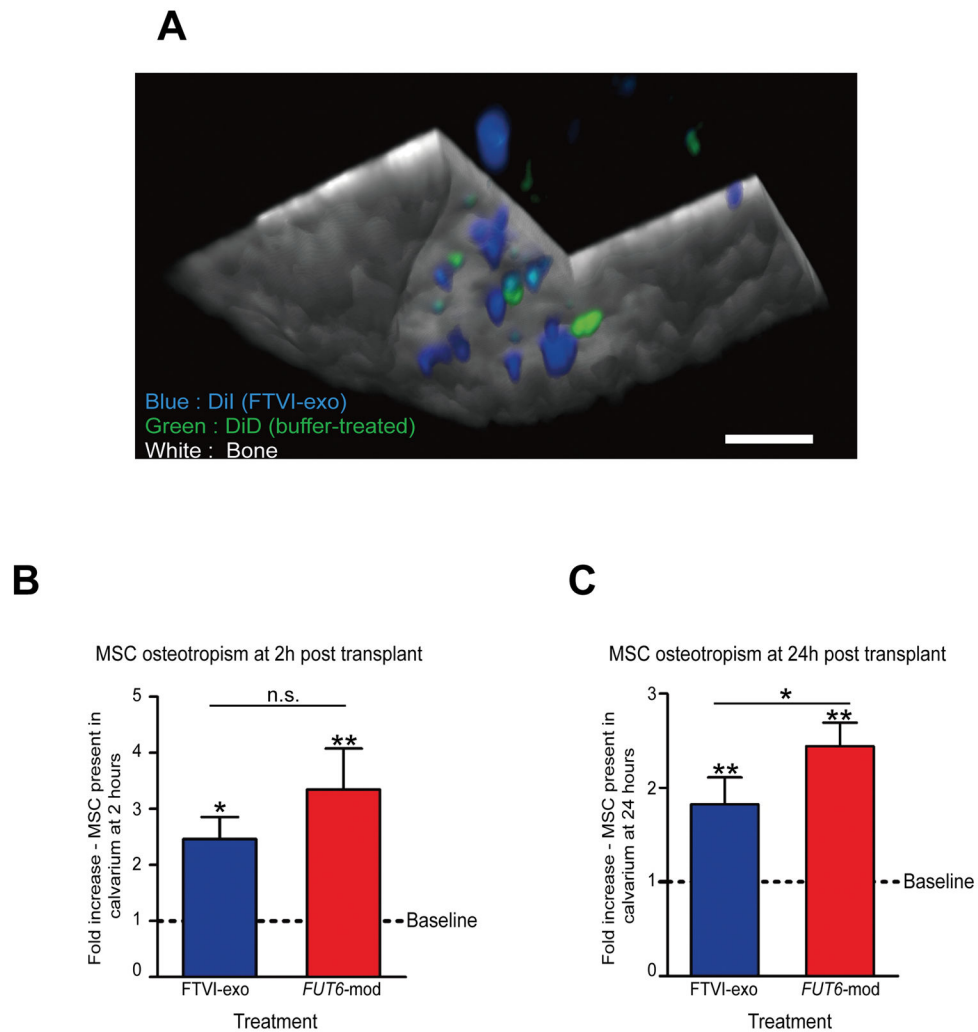


Figure 5. In vivo imaging of calvarial bone marrow to measure relative osteotropism of xenotransplanted human MSCs

(A) Three-dimensional reconstruction of mouse calvarium region after transplantation of DiD- (green) and DiI- (blue) stained MSCs. A portion of the bone is digitally removed to facilitate visualization of the bone marrow. Scale bar = 100 μ m. (B) Fucosylated human MSCs show increased osteotropism compared to control cells at 2 hours post-transplantation and (C) 24 hours post-transplantation, with intracellular fucosylation (*FUT6-mod*) yielding a stronger enhancement than extracellular fucosylation (FTVI-exo). Error bars = standard deviation. n=4 mouse pairs per comparison. Statistical comparisons were made using one-way ANOVA with Tukey's HSD test. * = $p < 0.05$; ** = $p < 0.01$.

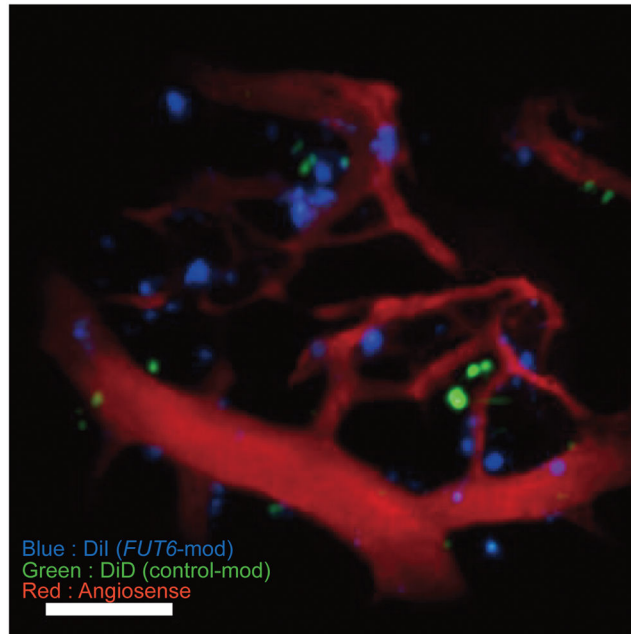
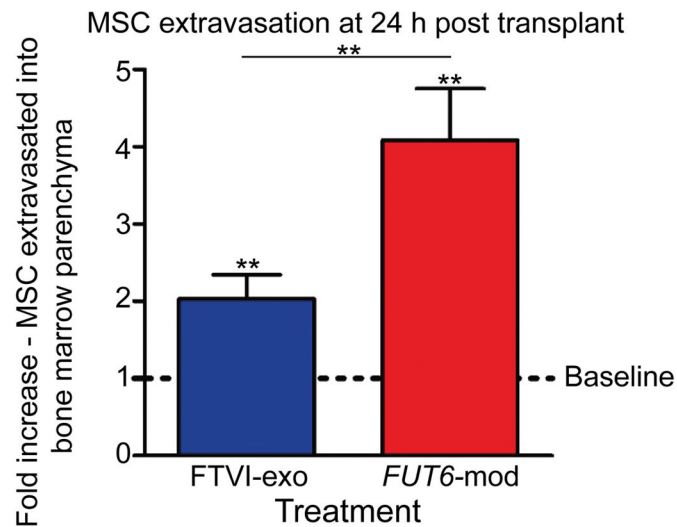
A**B**

Figure 6. In vivo imaging of blood vessels to measure extravasation of xenotransplanted human MSCs into bone marrow parenchyma

(A) 2D merged image stack of calvarium region after Angiosense injection to visualize blood vessels (red) and homed DiI- (blue) and DiD- (green) stained MSCs. Scale bar = 100 μ m. (B) Intracellularly fucosylated (*FUT6-mod*) MSCs show significantly greater MSC extravasation into bone marrow parenchyma than do extracellularly fucosylated (FTVI-exo) MSCs when compared to control cells (baseline) at 24 hours post-transplantation. Error bars = standard deviation. n=4 mouse pairs per comparison. Statistical comparisons were made using one-way ANOVA with Tukey's HSD test. ** = $p < 0.01$.